CG C 8

The Conjugate Beam Effective Thickness Method

Laura Galuppi [a], Adam J. Nizich [b], Andrea M. La Greca [c]

a   Department of Architecture and Engineering, University of Parma, Italy, laura.galuppi@unipr.it
b   Simpson Gumpertz & Heger Inc., Washington, DC, United States of America, ajnizich@sgh.com
c   Simpson Gumpertz & Heger Inc., Chicago, IL, United States of America, amlagreca@sgh.com

Abstract

The structural performance of laminated glass is strongly dependent on the shear coupling offered by the interlayer between the bounding layered and monolithic limits of the glass plies. The most common simplified design approach consists of defining the effective thickness, i.e., the thickness of a monolithic section with equivalent flexural section properties. The Enhanced Effective Thickness (EET) method has been verified to estimate deflection in laminated glass for a range of load and boundary conditions for two-, three-, and multi-ply beams; however, for some static schemes, the EET method is less accurate for predicting stress. The recently proposed Conjugate Beam Effective Thickness (CBET) method, initially developed for cantilevered laminated glass balustrade applications, accounts for the relative displacement of glass plies across the interlayer for a range of loads and statically determinate boundary conditions. In this paper, the CBET method is extended to the evaluation of two-ply simply supported beams under concentrated, uniformly, and tapered distributed out-of-plane loads. Predicted deflection- and stress-effective thickness obtained from effective thickness methods is compared with finite element model results in illustrative examples, demonstrating improved accuracy. Closed-form formulas are summarized in tables to facilitate the practical application of the CBET method in the design practice.

Keywords

Glass, Laminated Glass, Effective Thickness, Structural Analysis

Article Information

1. Introduction

Laminated Glass (LG) is a composite material formed by two or more glass plies bonded with a polymeric interlayer(s) to achieve the desired stiffness, strength, and reliability. LG stiffness and strength are governed by the *shear coupling* of the polymer between the glass plies, as first mentioned by Hooper (1973), and a function of the section properties and external load and boundary conditions, as highlighted by Galuppi and Royer-Carfagni (2012).

LG beams in flexure have a varying distribution of internal flexural and axial forces, depending on the interlayer shear modulus, G. As observed in Figure 1, for a simply supported LG beam with a concentrated load, the stress distribution on the tensile surface of the beam from axial and flexural forces is hyperbolic between the bounding layered (where $G \to 0$) and monolithic (where $G \to \infty$) limits. The conjugate beam analogy proposed by Galuppi and Royer-Carfagni (2020) allows for the determination of ply surface stresses based on the precise evaluation of axial forces in two glass plies, due to the shear stress transmitted by the interlayer, as observed in Figure 2.
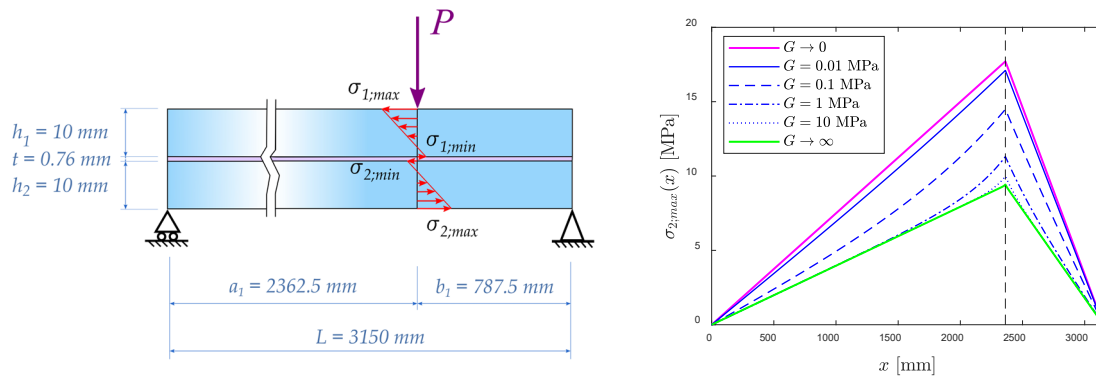

Fig. 1: An LG beam[1] with a concentrated load: Stress distribution across glass plies of a simply supported beam (left), maximum surface stress $\sigma_{2;\,max}$ along the length of the beam for different values of interlayer shear modulus (right).
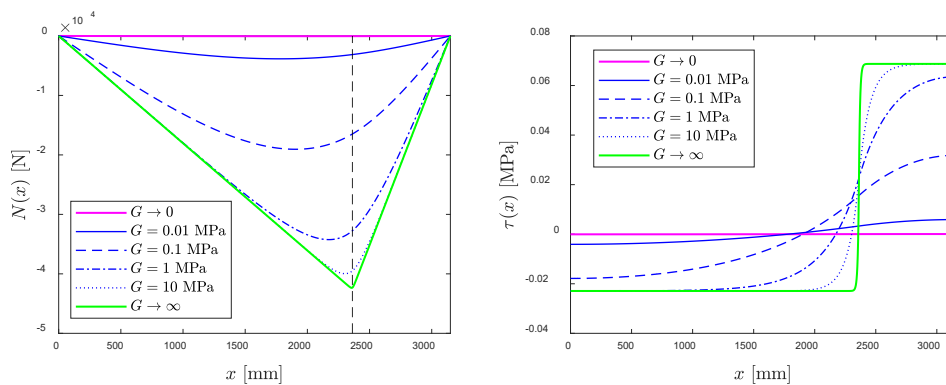

Fig. 2: Axial force (left) and interlayer shear stress (right) diagrams of the LG beam in Figure 1.

The complex structural mechanics of an LG beam can be simplified into a monolithic section with an *Effective Thickness* (ET) for evaluation with classical beam analysis equations corresponding to the associated loading and boundary conditions. Various effective thickness formulations have been proposed for the design of LG in flexure. The most well-known effective thickness methods are: (a) the

---

[1] Assumed structural parameters for the beam are L = 3150 mm, b = 1000 mm, $h_1 = h_2$ = 10 mm, t = 0.76 mm, E = 70.0 GPa, with a P = 1 kN concentrated load distributed across the width and through the lite thickness.

Wölfel-Bennison effective thickness method recorded in ASTM E1300 (2016), based on formulas derived by Bennison and others (Calderone et al. 2009) following the seminal work by Wölfel (1987), and (b) the Enhanced Effective Thickness (EET) method for beams proposed by Galuppi and Royer-Carfagni (2012) and Galuppi et al. (2013). These methods have limitations for evaluation of stress-ET for concentrated loads, and for evaluation of deflection- and stress-ET where slip occurs between plies in cantilever support conditions (Nizich and Galuppi 2019).

The *Conjugate Beam Effective Thickness* (CBET) method for cantilevered LG balustrades was recently proposed by Galuppi and Nizich (2021) and compared to existing effective thickness models by Nizich and Galuppi (2022). For the application of cantilevered LG supported in a conventional U-profile, particular attention was given to constrained and unconstrained slip between two glass plies at the support. Here, the method is extended to simply supported LG beams under concentrated, uniformly, and tapered distributed loads.

2. Effective Thickness Models

The method consists of defining the LG effective thickness (i.e., the thickness of a monolithic section with equivalent flexural section properties) between the bounding layered and monolithic limits. The reference geometry, shown in Figure 3, is a LG beam of width b, composed of two glass plies with a Young's modulus E and thickness h_1 and h_2, respectively, bonded by an interlayer of thickness $t \ll h_1, h_2$, with a shear modulus G.
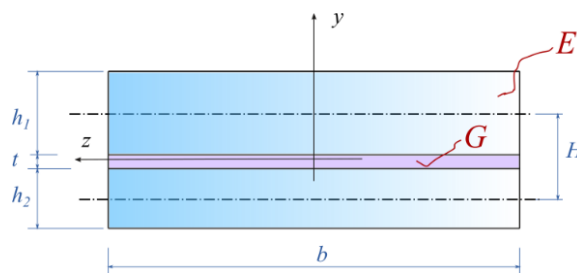

Fig. 3: A two-ply laminated glass beam section.

With reference to Figure 3, the section properties are defined as:

$$A_i = h_i b, \ I_i = \frac{bh_i^3}{12} \ (i = 1,2), \quad H = t + \frac{h_1 + h_2}{2}, \quad A^* = \frac{A_1 A_2}{A_1 + A_2}, \ I_L = I_1 + I_2, \ I_M = I_L + A^* H^2, \tag{1}$$

where I_L and I_M are the moment of inertia of the beam at the layered and monolithic limits, respectively.

2.1. Enhanced Effective Thickness Method

The Enhanced Effective Thickness (EET) method assumes that the deflection of a LG beam has the same shape as that of a monolithic beam subjected to the same boundary and loading conditions, with an *effective* inertia I_{ef}, being the weighted harmonic mean of the moment of inertia at the layered I_L and monolithic I_M limits. Under this assumption, the optimal response of the LG beam is evaluated, in a variational framework, by minimizing the total energy. This method is described in the Italian Glass Code CNR-DT 210 (2013), appears in the draft of the upcoming Eurocode on structural glass CEN/TS 19100-2 (2021), and has been extended to three- and multi-ply LG beams (Galuppi and Royer-Carfagni

2014) with equivalent accuracy. According to the EET model, the deflection- and stress-ET, for a two-ply LG beam may be evaluated as:
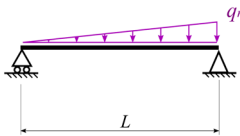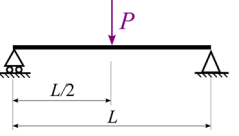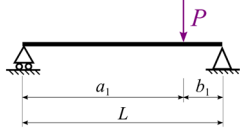
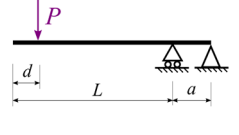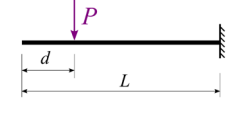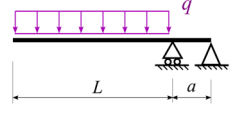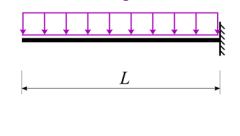$$h_{w;EET} = \left[\frac{b}{12}\left(\frac{\eta}{I_M} + \frac{1-\eta}{I_L}\right)\right]^{-\frac{1}{3}}, \quad h_{\sigma,i;EET} = \left[\frac{b}{12}\frac{2\eta\,I_i}{I_M} + \frac{h_i}{h_{w;EET}^3}\right]^{-\frac{1}{2}}, \tag{2}$$

where $\eta \in [0,1]$ is the nondimensional shear coupling coefficient, which corresponds to the beam's geometry, loading and boundary conditions, and glass and interlayer mechanical properties, evaluated as:

$$\eta = \frac{1}{1 + \dfrac{Et}{G}\dfrac{h_1 h_2}{h_1 + h_2}\dfrac{I_L}{I_M}\psi}. \tag{3}$$

The coefficient accounting for the boundary and load conditions of the beam Ψ is tabulated in Table 1 for select applications, as evaluated by Galuppi et al. (2013) for traditional combinations of loading and boundary conditions, and by Nizich and Galuppi (2022) for cantilevered LG balustrades, e.g., for cantilevered beams with a fixed end support as well as overhanging one support under different loading conditions.

Table 1: Values of EET loading and boundary condition coefficient Ψ for laminated glass beams.
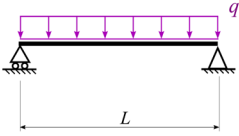
Loading and Boundary Conditions	Ψ	Loading and Boundary Conditions	Ψ
	$\dfrac{168}{17\,L^2}$		$\dfrac{10}{L^2}$
	$\dfrac{10}{L^2}$		$\dfrac{15}{L^2 + 2\,a_1 b_1}$
	$\dfrac{15}{6L^2 + 4La + a^2}$		$\dfrac{5}{2L^2}$
	$\dfrac{60(L + a - d)}{f(a, d, L)}$		$\dfrac{20}{(L-d)(8L + 7d)}$
	$\dfrac{42(3L + 5a)}{45L^3 + 105L^2 a + 70La^2 + 14a^3}$		$\dfrac{14}{5L^2}$
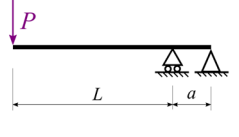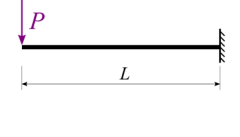
$$f(a, d, L) = 24L^3 + 40L^2 a - 27L^2 d + 20La^2 - 20Lad - 18Ld^2 + 4a^3 - 20ad^2 + 21d^3$$

The EET method has demonstrated adaptability to variations of load and boundary conditions for beams in flexure. However, as discussed by Nizich and Galuppi (2022), the traditional EET approach cannot account for the possibility of rigid axial displacement of one glass ply with respect to the other, affecting the interlayer shear strain and, consequently, the shear coupling and the LG beam flexural response. Its accuracy decreases in applications with asymmetric boundary conditions, point loads, and/or where relative displacement between glass plies does not equal zero at a known position (e.g., at a beam-end, midspan, etc.).

2.2. Conjugate Beam Effective Thickness Method

The CBET method recently proposed by Galuppi and Nizich (2021) is based on the conjugate beam analogy proposed by Galuppi and Royer-Carfagni (2020). According to the conjugate beam analogy, the axial force (equal and opposite in the two glass plies) is related to the external bending moment $M(x)$ by:

$$N''(x) - \alpha^2\mu^2 N(x) = \alpha^2(\mu^2 - 1)\frac{M(x)}{H}, \quad \mu = \sqrt{\frac{I_M}{I_L}}, \quad \alpha = \sqrt{\frac{Gb}{tEA^*}}. \tag{4}$$

As defined, μ is a geometrical nondimensional square root of the ratio of monolithic and layered limits, dependent on h_1, h_2, and t, while α also depends on the mechanical properties of both glass and the interlayer. The shear stress τ transmitted by the interlayer is related to the axial force by:

$$\tau(x) = \frac{1}{b}\frac{dN(x)}{dx}. \tag{5}$$

At the layered limit, the axial force is null, corresponding to null shear stress transmitted by the interlayer.

Galuppi and Royer-Carfagni (2020) demonstrated that the axial force $N(x)$ corresponds to the deflection of a conjugate beam subjected to a transverse load, indicated as $\tilde{w}$ in Figure 4, similar in shape to that load acting on the LG beam, and to a tensile axial force $\tilde{P}$, both dependent on the shear coupling. The boundary conditions for the conjugate beam depends not only on the support conditions for the laminate, but also on the axial constraints for slip between the two glass plies. This analogy allows evaluation of the axial force and shear coupling of the LG beam, simply by studying the deflection of the conjugate beam (Figure 4). Indeed, the axial force $N(x)$ corresponds to the deflection of the conjugate beam at x, while the shear stress $\tau(x)$ is the slope of the elastic curve of the conjugate beam at the same point.
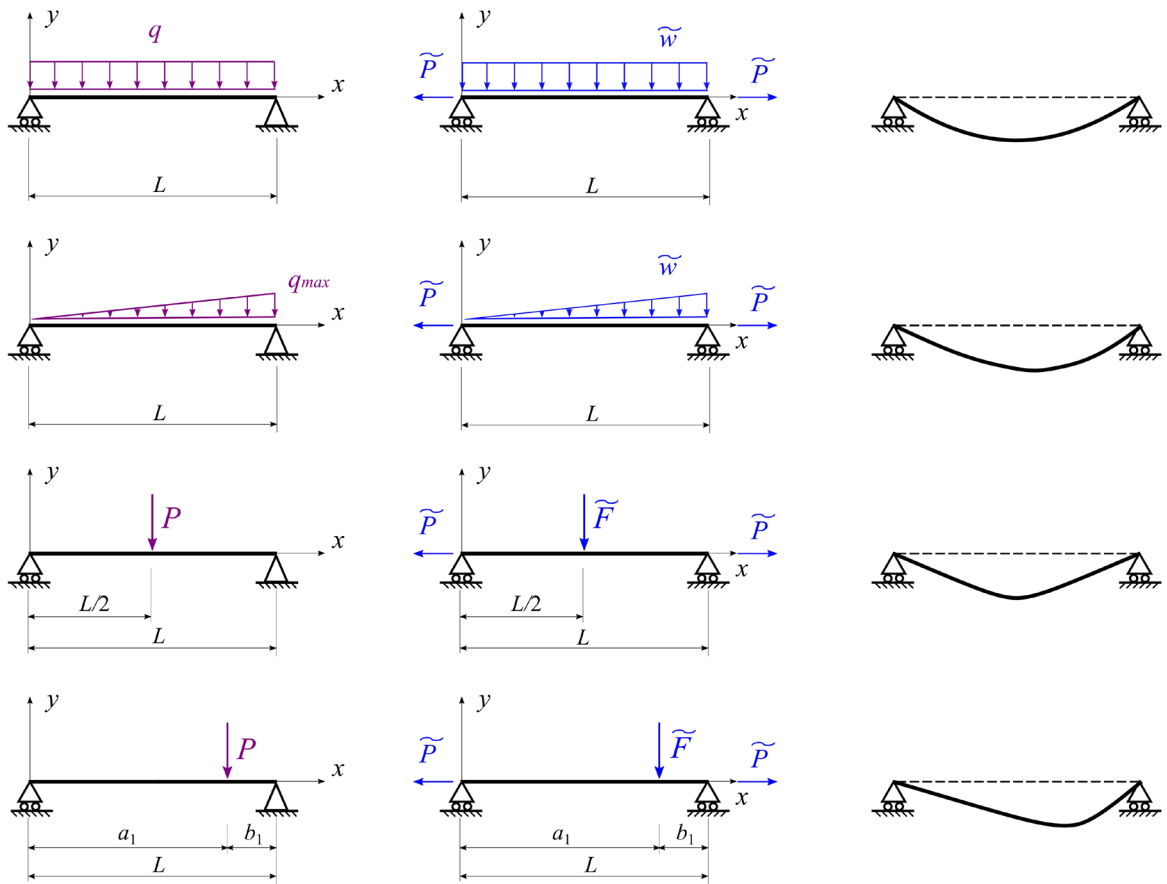
Fig. 4: Beam with actual loads (left), conjugate beam with fictitious loads (middle), and qualitative deformed shape of the conjugate beam (right).

Once the axial load is evaluated by means of the conjugate beam analogy (Eq. 4), this may be used to evaluate the effective thickness of the LG beam.

2.2.1. Deflection-Effective Thickness

The deflection of the LG beam corresponds to the deflection of a beam with moment of inertia I_L, subjected to a *fictitious* bending moment (accounting for the shear stress transmitted by the interlayer) equal to $M(x) + N(x)H$. Hence, the deflection $v(x)$ may be calculated by solving the differential equation:

$$EI_L v''(x) = M(x) + N(x)H,$$
(6)

with appropriate boundary conditions. To find the deflection-ET (h_w), $v(x)$ must be compared with the maximum deflection of an equivalent monolithic beam, of thickness h_w and inertia $I_{ef} = b\, h_w^3/12$, i.e., with the solution of:

$$EI_{ef} v''_{ef}(x) = M(x).$$
(7)

Since the deflection of the two beams are different in shape, because they are subjected to qualitatively different bending moments, the comparison is made in terms of their maximum values. It may be verified that this provides a deflection-ET formula in the form of:

$$I_{ef} = \frac{I_M}{1 + \frac{I_M - I_L}{I_M} \cdot \beta \cdot (1 - \lambda_w)}, \tag{8}$$

$$h_w = \sqrt[3]{\frac{12\, I_{ef}}{b}}, \tag{9}$$

where geometric (β) and coupling (λ_w) coefficients are dependent on the loading and boundary conditions, recorded in Table 2. The effective laminate thickness approaches the equivalent monolithic limit for stiff interlayers where $\lambda_w \to 0$.

2.2.2. Stress-Effective Thickness

The *i*-th glass ply ($i = 1, 2$) is subjected to a part of the *fictitious* bending moment, proportional to its inertia, and to the axial force $N(x)$. Its surface stress could be hence evaluated as:

$$\sigma_i(x) = \frac{M(x) + N(x)H}{I_L}\frac{h_i}{2} \pm \frac{N(x)}{A_i}, \tag{10}$$

To evaluate the corresponding stress-effective thickness, this value is compared with the maximum stress acting in a monolithic effective beam of thickness $h_{\sigma;i}$, subjected to the same bending moment $M(x)$ of the LG element, which is:
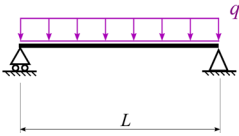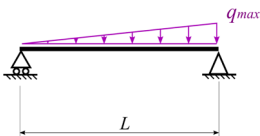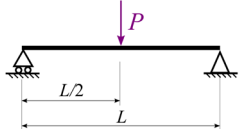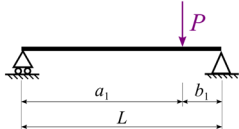
$$\sigma_{ef;i}(x) = \frac{6M(x)}{bh_{\sigma;i}^2}. \tag{11}$$

Again, due to the different shape of bending moment and normal force, the maximum stresses $\sigma_i(x)$ and $\sigma_{ef;i}(x)$ could be locate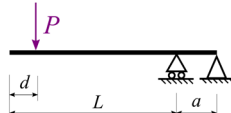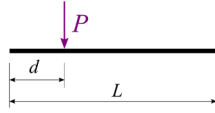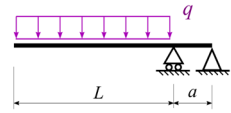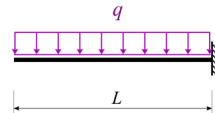d at different locations x along the beam, and the comparison should be made in terms of their maximum value. Therefore, the coupling coefficient for stress λ_σ can be different from λ_w, when the maximum LG stress and effective-stress occur at different locations, as recorded in Table 2. Nizich and Galuppi 2022 verified that this provides stress-ET formula in the form:

$$h_{\sigma;i} = \sqrt{\frac{6I_M}{\frac{b\,h_i}{2} \cdot \left(1 + \lambda_\sigma \cdot \frac{I_M - I_L}{I_L}\right) + \frac{(I_M - I_L)(1 - \lambda_\sigma)}{H \cdot h_i}}}. \tag{12}$$

The CBET method was originally developed to address the structural performance of cantilevered LG balustrades. Here, the CBET method is applied to the analysis of simply supported LG beams under concentrated, uniformly distributed, and tapered distributed loads.

Table 2: Values of CBET coefficients β and λ for laminated glass beams under different loading and boundary conditions

Loading and Boundary Conditions	Geometric (β) and Coupling ($\lambda_w, \lambda_\sigma$) Coefficients

$$\beta = \frac{48}{5\,\alpha^2\,L^2}, \qquad \lambda_w = \lambda_\sigma = \frac{8\left[1 - \dfrac{1}{cosh(0.5\alpha\mu L)}\right]}{\alpha^2\,\mu^2\,L^2}$$

$$\beta = \frac{15\sqrt{30}}{L^2\,\alpha^2\,(3+\sqrt{30})}, \qquad \lambda_\sigma = \frac{9}{\alpha^2\,\mu^2\,L^2}\left(1 - \frac{sinh\left(\frac{1}{3}\alpha\mu L\sqrt{3}\right)\sqrt{3}}{sinh(\alpha\mu L)}\right)$$

$$\lambda_w = \frac{3}{2}\frac{\sqrt{30}}{\alpha^2\,\mu^2\,L^2}\left(1 - \frac{sinh\left(\frac{1}{15}\alpha\mu L\sqrt{225-30\sqrt{30}}\right)15}{sinh(\alpha\mu L)\sqrt{225-30\sqrt{30}}}\right)$$

$$\beta = \frac{12}{\alpha^2\,L^2}, \qquad \lambda_w = \lambda_\sigma = -\frac{2\left(1 - cosh(\alpha\mu L)\right)}{sinh(\alpha\mu L)\alpha\mu L}$$

Where $a_1 \geq b_1$

$$\beta = \frac{9}{\alpha^2\,a_1\,(a_1+2b_1)}, \qquad \lambda_\sigma = \frac{sinh(\alpha\mu b_1)\,sinh(\alpha\mu a_1)L}{sinh(\alpha\mu L)\,\alpha\,\mu\,a_1 b_1}$$

$$\lambda_w = \frac{sinh(\alpha\mu b_1)\,sinh\left(\frac{1}{3}\alpha\mu\sqrt{3}\sqrt{a_1\,(a_1+2b_1)}\right)\sqrt{3}\,L}{sinh(\alpha\mu L)\,\alpha\mu b_1\,\sqrt{a_1\,(a_1+2b_1)}}$$

$$\beta = \frac{3}{\alpha^2\,a\,L}, \qquad \lambda_w = \lambda_\sigma = \frac{(L+a)\cdot sinh(\alpha\mu a)\cdot sinh(\alpha\mu L)}{\alpha\mu a L\cdot sinh\left(\alpha\mu\cdot(L+a)\right)}$$

$$\beta = \frac{3}{\alpha^2\,L^2}, \qquad \lambda_w = \lambda_\sigma = \frac{tanh(\alpha\mu L)}{\alpha\mu L}$$

$$\beta = \frac{6\,(L+a)}{\alpha^2\,a\,(2\,L^2+2L\,a-L\,d-d^2)},$$

$$\lambda_w = \lambda_\sigma = \frac{sinh(\alpha\mu a)}{sinh\left(\alpha\mu\cdot(L+a)\right)\cdot\alpha\mu\cdot(L-d)}\left[\frac{(L+a-d)sinh(\alpha\mu L)}{a} - sinh(\alpha\mu d)\right]$$

$$\beta = \frac{6}{\alpha^2(2\,L+d)(L-d)}, \qquad \lambda_w = \lambda_\sigma = \frac{sinh(\alpha\mu L)-sinh(\alpha\mu d)}{\alpha\mu(L-d)\,cosh(\alpha\mu L)}$$

$$\beta = \frac{12\,(L+a)}{\alpha^2\,L\,a\,(3L+4a)},$$

$$\lambda_w = \lambda_\sigma = \frac{sinh(\alpha\mu a)}{sinh\left(\alpha\mu\cdot(L+a)\right)\alpha^2\mu^2 L^2}\left[\alpha\mu L\cdot sinh(\alpha\mu L)\left(\frac{L}{a}+2\right)-2\left(cosh(\alpha\mu L)\right)\right.$$
$$\left.-1\right]$$

$$\beta = \frac{4}{\alpha^2\,L^2}, \qquad \lambda_w = \lambda_\sigma = \frac{2}{\alpha^2\mu^2 L^2}\left[\frac{\alpha\mu L\,sinh(\alpha\mu L)+1}{cosh(\alpha\mu L)}-1\right]$$

3. Evaluation and Comparison

To compare the analytical effective thickness models, numerical analyses have been performed with Strand7 (2021), by modeling the LG beam as a 2D sandwich section, using four-noded plane-stress finite elements. The mesh was scaled proportional to the interlayer thickness and elements maintained a maximum aspect ratio of 2:1, with three subdivisions through the interlayer thickness. Loads and boundary conditions were applied in accordance with the modeling and analysis criteria discussed by Nizich and Galuppi (2022).

To perform accurate comparison of detailed 2D numerical models with the analytical beam models, concentrated forces (representative of a quasi-concentrated load) are distributed through the thickness of glass section, thus avoiding a nodal stress concentration. Evaluated models are representative of more complex 3D applications; marginal differences are expected and are in general agreement with engineering theory.

3.1. Simply Supported LG Beam Example

The beam section, length, and loads used for original comparison of the EET method with a numerical model (Galuppi and Royer-Carfagni 2012) are adopted for the four simply supported beam load cases represented in Figure 3. Assumed structural parameters for all cases are L = 3150 mm, b = 1000 mm, $h_1 = h_2 = 10$ mm, $t = 0.76$ mm, E = 70.0 GPa, while the shear modulus G of the interlayer is varied to evaluate its influence on the shear-coupling of the glass plies. The distributed beam load, q, is 0.75 N/mm, equivalent to 0.75 kPa. The point load is 1 kN.
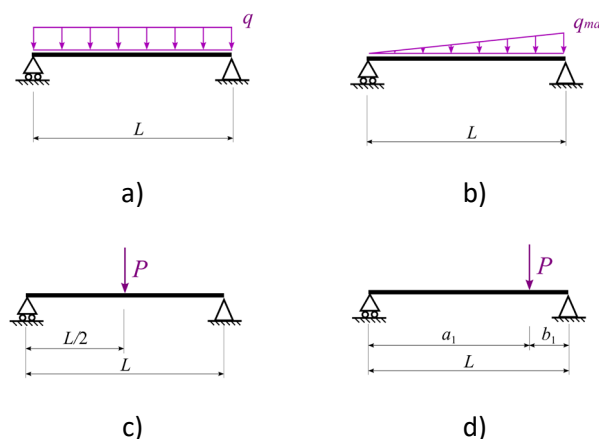

Fig. 5: Representative examples of laminated glass beams under different boundary and load conditions.

In Figures 6 – 9 below, deflection- and stress-effective thickness for each beam are compared, as bounded by the layered and monolithic limits. We observe good correlation of the EET, CBET, and numerical methods for the distributed load cases in Figures 6 and 7. Indeed, further accuracy in comparison to the numerical model is obtained with the CBET method.
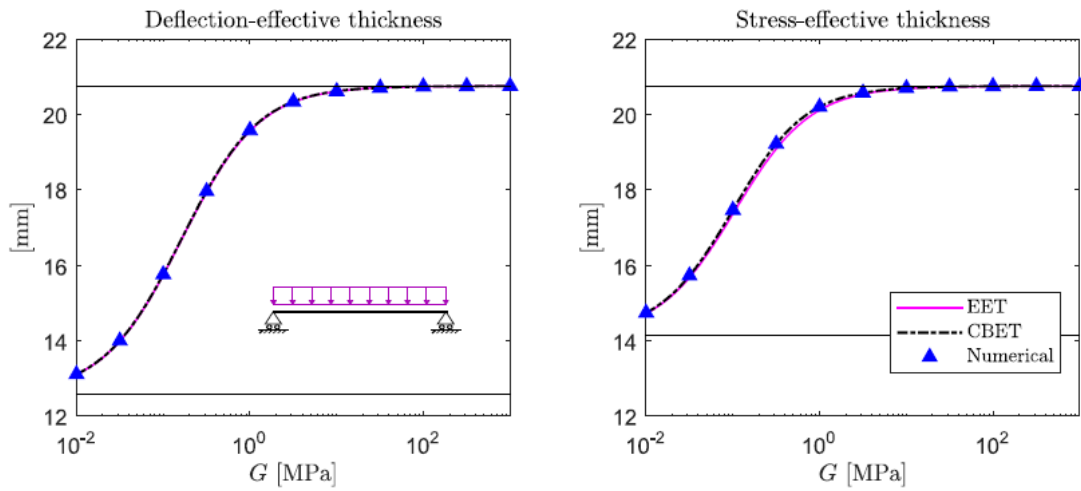
Fig. 6: Deflection- (left) and stress-ET (right) for a simply supported LG beam with a uniformly distributed load. Numerical results compared to ET methods.
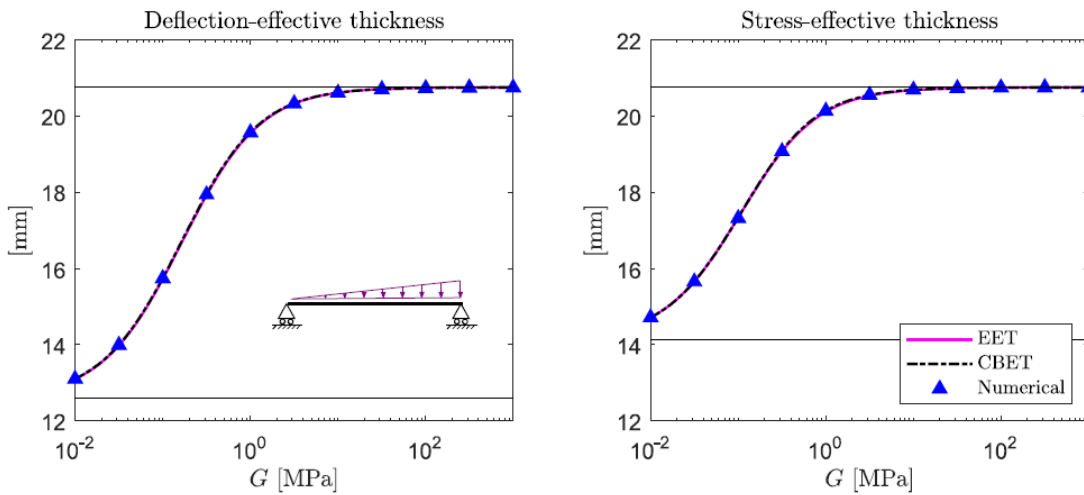

Fig. 7: Deflection- (left) and stress-ET (right) for a simply supported LG beam with a uniformly tapered distributed load. Numerical results compared to ET methods.

For point load cases in Figures 8 and 9, we observe good correlation of the EET, CBET, and numerical methods for deflection-ET. Significant deviation of stress-ET is observed between the EET and CBET methods. Remarkably, the numerical results coincide with the CBET method.
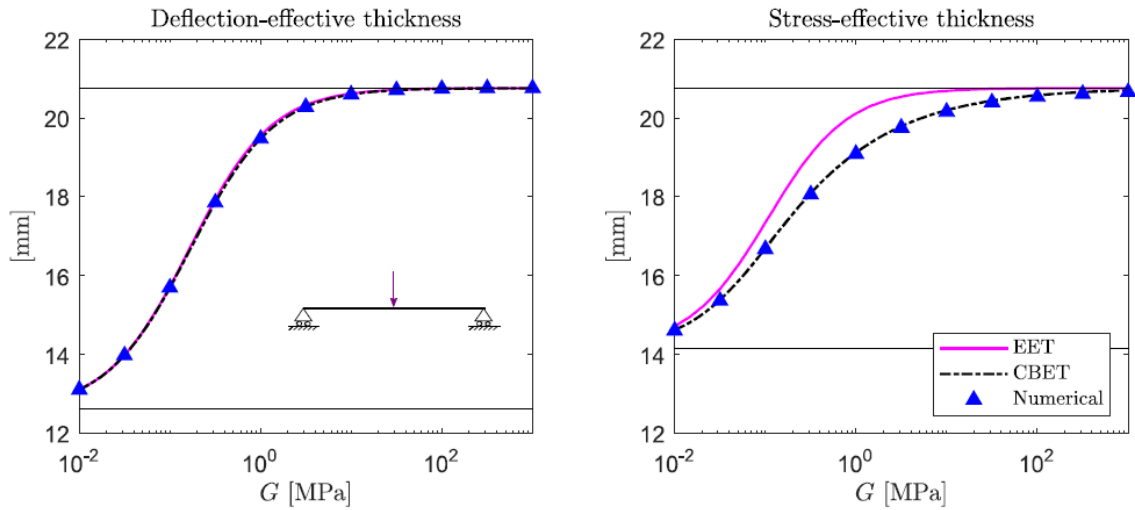
Fig. 8: Deflection- (left) and stress-ET (right) for a simply supported LG beam with a point load at midspan. Numerical results compared to ET methods.
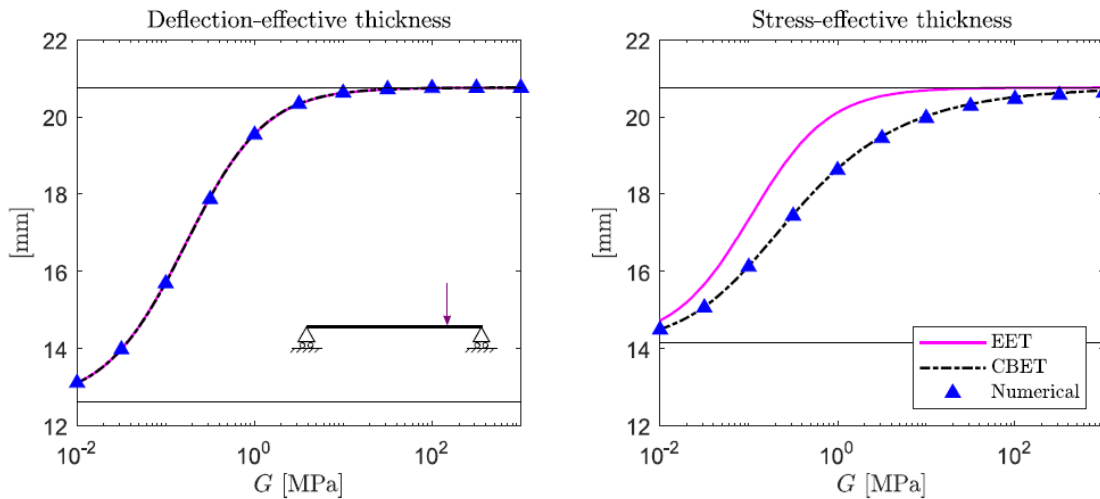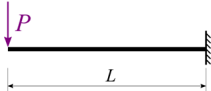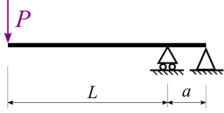

Fig. 9: Deflection- (left) and stress-ET (right) for a simply supported LG beam with a point load at quarter span. Numerical results compared to ET methods.

3.2. Cantilevered LG Beam Example

Many cantilevered laminated glass balustrades with an approximate L = 1100 mm cantilever free length have been constructed with a pair of fully tempered 6 mm plies (nominal thickness) around a 1.52 mm interlayer to resist live loads. We compare the effective thickness for this geometry for two cantilevered beam support conditions in Table 3 and evaluate deflection and stress using classical formulas for the corresponding loading and boundary conditions. Assumed structural parameters for all cases are: L = 1100 mm, a = 50 mm, b = 1500 mm, $h_1 = h_2$ = 5.56 mm, t = 1.52 mm, and E = 71.7 GPa as per the minimum thickness and mechanical properties in ASTM E1300. A 0.73 kN/m service level design load (unfactored) is applied to the free end of the beam as a P = 1.095 kN point load.

Table 3: Classical formulae of maximum deflection δ_{max} and stress $\sigma_{i;max}$ for cantilever beams with a point load at the free end under boundary conditions.

Loading and Boundary Conditions		δ_{max} (at the free end)	$|\sigma_{i;max}|$
Case i) fixed end support		$\dfrac{P\,L^3}{3\,E\,I_{ef}}$	$\dfrac{6\,P\,L}{b\,h_{i;\sigma}{}^2}$
Case ii) overhanging one support		$\dfrac{P\,L^2\,(L+a)}{3\,E\,I_{ef}}$	$\dfrac{6\,P\,L}{b\,h_{i;\sigma}{}^2}$

In Figure 10 below, deflection- and stress-effective thickness for each support condition is compared. We observe good correlation of the EET, CBET, and numerical methods of deflection-ET for a fixed end support (case i), however, only the CBET method predicts the response of for a beam overhanging one support (case ii).
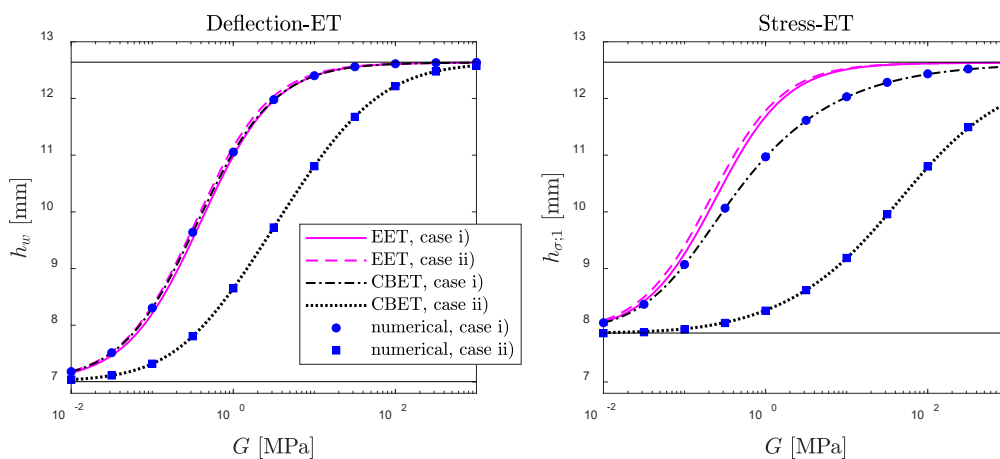

Fig. 10: Deflection- (left) and stress-ET (right) for a cantilevered LG beam with a point load at the free end evaluated for two support conditions. Numerical results compared to ET methods.

In Figure 11, we observe a significant difference in the predicted deflection and stress between the two idealized support cases, corresponding to the classical beam equations in Table 3.
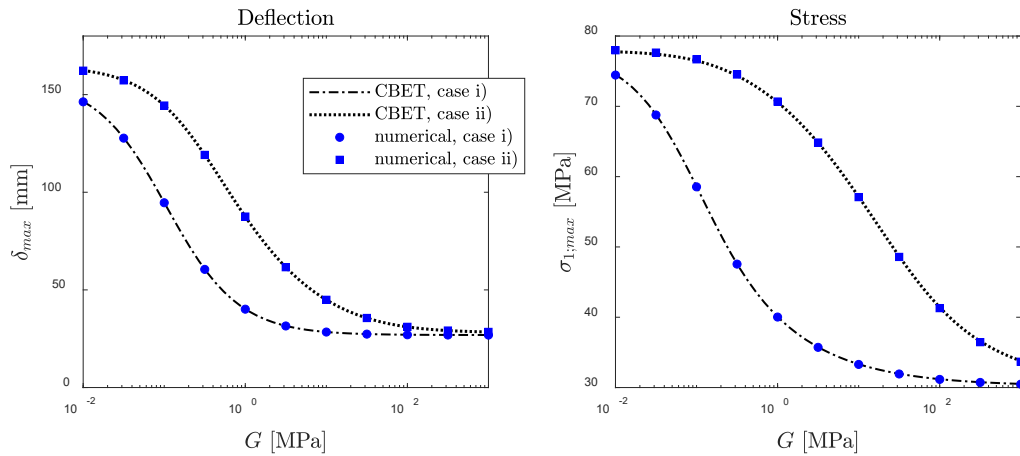
Fig. 11: Deflection (left) and surface stress (right) for a cantilevered LG beam with a point load at the free end evaluated for two support conditions. Numerical results compared to ET methods.

A fixed-end support (Case i) implies that the plies are constrained from relative slip at the support. Given that many balustrades are installed with nonadhesive grouts, or discrete wedge blocks, we assume that a slip-critical connection is generally not developed in conventional installations. If a fixed-end support boundary condition is assumed, and not realized in construction, the predicted deflection is at risk of increasing by 118% and maximum surface stress by 82% to perform as a cantilevered beam overhanging one support (Case ii) for the evaluated conditions. Variations in deflection, glass stress, and interlayer shear strain for different supports are observable in a 3D-layered finite element model (Figure 12) with an interlayer shear stiffness of G = 10 MPa.
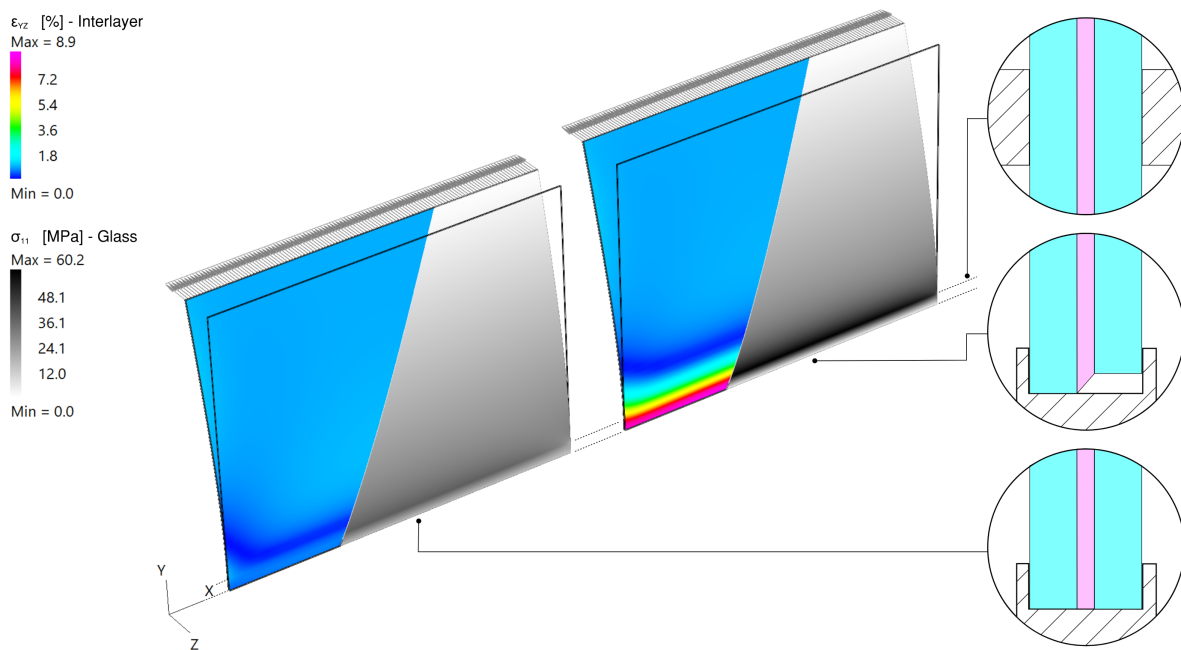

Fig. 12: Cutaway of a cantilevered LG balustrade with support that constraints slip between plies at the support (left), and support that allows slip (right). Interlayer shear strain ε_{yz} and glass maximum principal surface stress σ_{11} are plotted on the deformed shape.

4. Current Work

Task groups within the ASTM E06.52 subcommittee and the European Committee for Standardization (CEN/TS 2021) are currently collaborating on new structural glass standards. In support of this work, a new ASTM standard for the effective thickness evaluation of laminated glass is under preparation to encompass methods for assessment of flexural and torsional section properties in two-, three-, and multi-ply LG sections.

5. Conclusion

The Conjugate Beam Effective Thickness (CBET) method has been verified for both uniformly distributed and concentrated loads for a range of statically determinate beam boundary conditions, applicable to the design of one- and two-edge supported glass. The method is simple to use and allows for evaluation of deflection and stress with classical engineering beam equations. Recent advances in effective thickness methods can inform the discussion on design strength for laminated glass and inform the development of structural glass building codes.

References

ASTM E1300-16: Standard practice for determining load resistance of glass in buildings. ASTM Int. 2016. https://doi.org/10.1520/E1300-16

Calderone, I., Davies, P.S., Bennison, S.J., Xiaokun, H., Gang, L.: Effective laminate thickness for the design of laminated glass. In Proceedings of Glass Performance Days, Tampere (FI), 12–15, (2009)

CEN/TS 19100-2:2021: Design of glass structures – Part 2: Design of out-of-plane loaded glass components. European Committee for Standardization, (2021)

CNR-DT 210: Guide for the Design, Construction and Control of Buildings with Structural Glass Elements. National Research Council, Italy, (2013)

Galuppi, L., Manara, G., Royer Carfagni, G.: Practical expressions for the design of laminated glass. Composites Part B: Engineering, 45.1, 1677–1688, (2013). https://doi.org/10.1016/j.compositesb.2012.09.073

Galuppi, L., Nizich, A.J.: Cantilevered laminated glass balustrades: the Conjugate Beam Effective Thickness method—part I: the analytical model. Glass. Struct. Eng. 6, 377–395 (2021). https://doi.org/10.1007/s40940-021-00156-8

Galuppi, L., Royer-Carfagni, G.: Effective thickness of laminated glass beams. New expression via a variational approach. J. Eng. Struct. 38, 56–67 (2012). https://doi.org/10.1016/j.engstruct.2011.12.039

Galuppi, L., Royer-Carfagni, G.: Enhanced Effective Thickness of multi-layered laminated glass. Composites Part B: Engineering, 64, 202-213, (2014). https://doi.org/10.1016/j.compositesb.2014.04.018

Galuppi, L., Royer-Carfagni, G.: Conjugate-beam analogy for inflexed laminates. Int. J. Sol. Struct., 206, 396-411, (2020). https://doi.org/10.1016/j.ijsolstr.2020.09.020

Hooper, J.A.: On the bending of architectural laminated glass. Int. J. Mech. Sci. 15, 309–23, (1973). https://doi.org/10.1016/0020-7403(73)90012-X

Nizich, A.J., Galuppi, L.: Enhanced effective thickness method for cantilevered laminated glass balustrades. In Proceedings of Glass Performance Days, Tampere (FI), 398-401, (2019)

Nizich, A.J., Galuppi, L.: Cantilevered laminated glass balustrades: the Conjugate Beam Effective Thickness method—part II: comparison and application. Glass. Struct. Eng. (2022). https://doi.org/10.1007/s40940-021-00165-7

Strand7: Strand7 Finite Element Analysis System. Version 3.1.1. Strand7 Pty. Ltd. Sydney, (2021)

Wölfel, E.: Nachgiebiger verbund - eine näherungslösung und deren anwendungsmöglichkeiten. Stahlbau, 6:173-180, (1987)

CG C8

Platinum Sponsors

SAINT-GOBAIN

EASTMAN

Gold Sponsors

Bellapart

DOW

kuraray
Trosifol®
SentryGlas®

sedak

SEEN

Silver Sponsors

octatube

PERMASTEELISA GROUP

vitroplena
structural glass solutions

Organising Partners

GHENT UNIVERSITY

TU/e

TUDelft